Biophysical Characterization of Zinc Ejection from HIV Nucleocapsid Protein by Anti-HIV 2,2′-Dithiobis[benzamides] and Benzisothiazolones

Joseph A. Loo, Tod P. Holler, Joseph Sanchez, Rocco Gogliotti, Lisa Maloney, and Michael D. Reily*

Parke-Davis Pharmaceutical Research, Division of Warner Lambert Company, 2800 Plymouth Road, Ann Arbor, Michigan 48105

Received April 1, 1996[⊗]

HIV nucleocapsid protein (NCp7) has been suggested as a possible target for 2,2′-dithiobis-[benzamide] and benzisothiazolone agents that inhibit viral replication in infected cells (Rice et al. *Science* **1995**, *270*, 1194−1197). The solution behavior of these compounds and the mechanistic events leading to removal of Zn from HIV nucleocapsid protein *in vitro* has been studied by electrospray ionization mass spectrometry, 500 MHz one- and two-dimensional nuclear magnetic resonance spectroscopy, and circular dichroism spectroscopy. We demonstrate that (1) Zn ejection is accompanied by formation of covalent complexes formed between the 2,2′-dithiobis[benzamide] monomers and Cys residues of Zn-depleted NCp7, (2) the rate of Zn ejection is faster for the C-terminal Zn finger and slower for the N-terminal finger, (3) Zn ejection results in a loss of structural integrity of the NCp7 protein, and (4) there is no appreciable interaction between a nonreactive isostere of the lead 2,2′-dithiobis[benzamide] and NCp7 in buffered aqueous solution. These findings are discussed in terms of the mechanism of action of Zn ejection by aromatic 2,2′-dithiobis[benzamides].

Introduction

Processing products of retroviral *gag* polypeptides invariably include nucleocapsid (NC) proteins that contain one or two C-X2-C-X4-H-X4-C motifs which are involved in encapsulation of the genomic RNA prior to or during viral particle assembly. These motifs are known to bind Zn^{2+} with sub-picomolar affinities.[1] In HIV, the first 55 amino acids of the mature form of nucleocapsid protein, NCp7, have been shown to form Zn fingers in the presence of stoichiometric Zn^2 (see Chart 1). Certain oxidizing agents, including 3-nitrosobenzamides and cupric ions, cause removal of zinc from NCp7 *in vitro*.[3] Recently, it has also been shown that certain aromatic 2,2′-dithiobis[benzamides] and benzisothiazolone compounds, bearing the general structures shown (**2** and **3**), also induce extraction of Zn from the peptide[4−7] and possess anti-HIV activity.[8] A common structural feature of these agents is the presence of electron-poor sulfur atom(s), making it likely that the first step in Zn ejection is nucleophilic attack of the 2,2′-dithiobis[benzamide] or benzisothiazolone sulfur by a Zn-coordinated cysteine sulfur atom. Extensive biochemical characterization of structure−activity relationships (SAR) within this class of compounds has provided evidence that a recognition event may precede Zn ejection.[4−8] For example, the meta- and para-isomers of active compounds are inactive,[4,7,8] suggesting some importance of the three-dimensional structure of the active compounds. If such a recognition complex existed, it would provide an obvious starting point for structure-based drug design. It has also been suggested that NCp7 may be the *in vivo* target of these compounds based primarily on whole virion cross-linking studies, the lack of resistance development to any of these compounds, and the observation that 2,2′-dithiobis-[benzamides] which do not inhibit HIV infectivity also do not eject Zn *in vitro*.

Chart 1

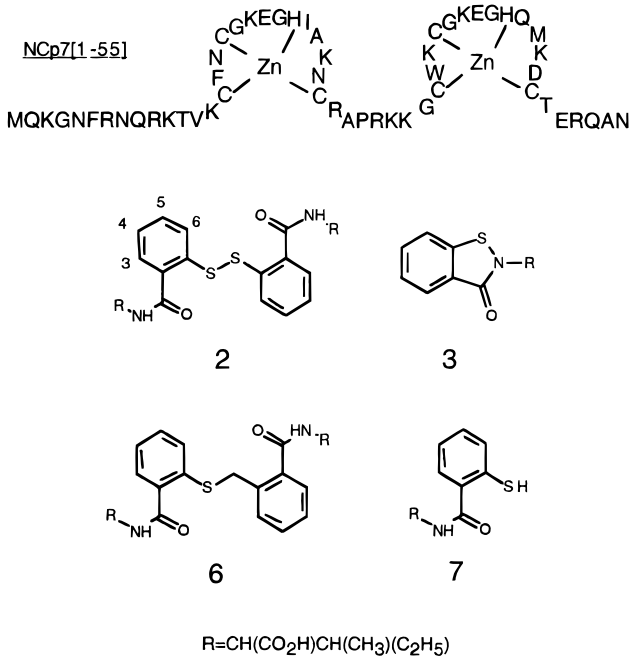

Work in this and other laboratories has recently been focused on elucidating the mechanism of action of these compounds.[4−8] This has been complicated by several factors including the potential for the 2,2′-dithiobis-[benzamides] to disproportionate into free sulfhydryl and benzisothiazolone forms and their ability to form mixed disulfides with endogenous thiols. In this report we investigate two active compounds, **2** and **3**, and a nonreactive thioether, **6** (see Chart 1). These compounds were evaluated for stability and their ability to remove Zn from HIV nucleocapsid protein *in vitro* using electrospray ionization mass spectrometry (ESI-MS), 500 MHz one- and two-dimensional nuclear magnetic resonance (NMR) spectroscopy, and circular dichroism (CD) spectroscopy.

* To whom correspondence should be addressed.
[⊗] Abstract published in *Advance ACS Abstracts,* September 1, 1996.

S0022-2623(96)00253-1 CCC: $12.00

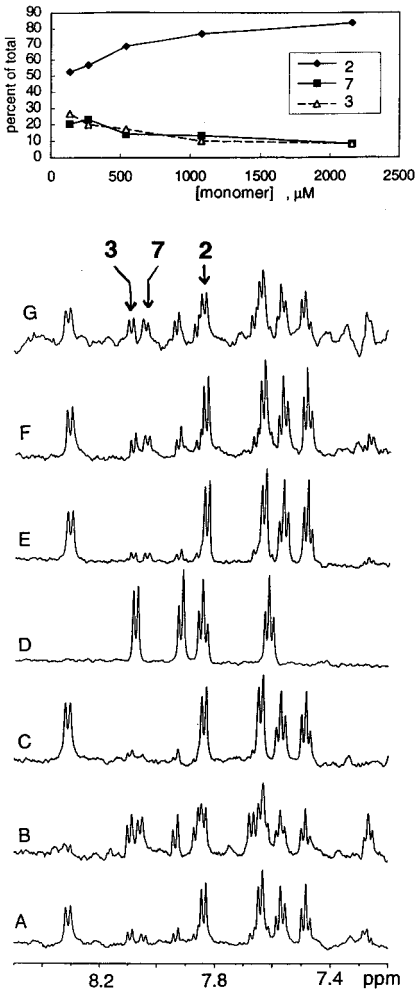

Figure 1. Effect of pH and concentration on the aromatic spectral regions of the 500 MHz ^{1}H NMR spectra of H_2O solutions of **2**. The H6 signal for each species is identified, and all other signals arise from the other aromatic and amide protons in each species. All concentrations are adjusted to reflect [monomer]: (A) 0.459 mM **2** at pH 7.4, 20 mM sodium phosphate buffer; (B) Sample in A raised to pH 8.5; (C) sample in B lowered to pH 6.6, the predominant signals in C are from the 2,2′-dithiobis[benzamide] **2**; (D) 2.93 mM **3** at pH 6.9, 20 mM sodium phosphate buffer, since **3** is stable in the absence of reducing agents, spectrum D provides a reference spectrum for **3** for purposes of comparison; (E) 2.16 mM **2** at pH 7.4, equilibrated for 40 min; (F) 4-fold dilution of E with H_2O; (G) 16-fold dilution of E with H_2O. Top: Relative amounts of dimeric and monomeric species present at various concentrations of **2** at pH 7.4. These data were extracted from aromatic signal peak heights as a function of concentration.

Results

Equilibrium Behavior of the 2,2′-Dithiobis[benzamides] in Solution. When dissolved in aqueous solution, many 2,2′-dithiobis[benzamides] reversibly disproportionate to form one molecule of mercaptan and one molecule of benzisothiazolone. The effect of pH and concentration on this equilibrium between **2** and its monomeric relatives (**3** and **7**), as monitored by the proton NMR spectrum, is shown in Figure 1. For these experiments, **2** was dissolved in buffer at various concentrations and pH's and the relative amounts of each species were determined by peak height after equilibrium was established. At pH 6.6 and 0.5−1.0 mM concentrations of **2**, the predominant species in solution is the dimer **2**. At similar concentrations at pH 7.4, **2** is still the major species with small amounts of the benzisothiazolone **3** and the thiol **7** present in solution. At pH 8.5, the equilibrium is pushed further, and **2** is the minor species in solution. Also, as the concentration is decreased at pH 7.4, the amount of **2** decreases with a concomitant increase in species **3** and **7**. Under all of the conditions studied, both **3** and **7** were present in approximately equal proportions.

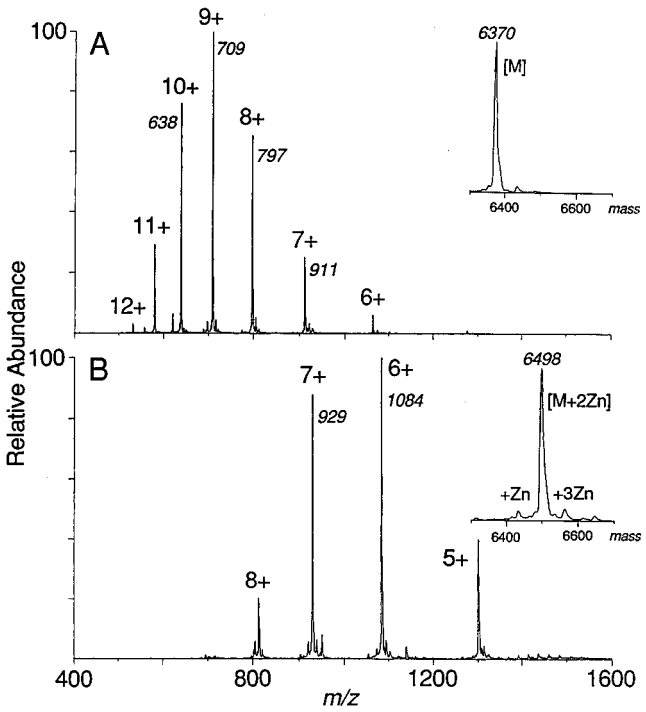

Figure 2. Effect of pH on zinc binding measured by ESI-MS. A 15 μM NCp7 solution containing 30 μM $ZnCl_2$ was prepared in 2:1 MeOH/H_2O with 2.5% (v/v) acetic acid (pH 2.5) (A) or 25 mM ammonium acetate, pH 6.9 (aqueous) (B) and analyzed by ESI-MS. Both the ESI-MS and the deconvoluted spectra (converted to the mass domain, inset) are shown. The spectrum acquired at pH 2.5 showed a measured mass of 6369.5 ± 0.4 Da, consistent for the apoprotein (theory 6369.5 Da). At pH 6.9, the dominant species is consistent for two zinc ions bound to the protein.

Characterization of Zn Ejection by Mass Spectrometry. The changes in mass of Zn-loaded NCp7 proved to be useful in characterizing Zn ejection. Electrospray ionization mass spectrometry has recently been used to study the metal-binding behavior of metalloproteins.[9] In particular, the zinc-binding characteristics of zinc finger protein glucocorticoid receptor DNA-binding domain[10] and nucleocapsid protein[11,12] have been studied using ESI-MS. Our studies with NCp7 are shown in the following examples. The ESI mass spectrum of a zinc-containing solution of NCp7 in 2:1 methanol/water with 2.5% (v/v) acetic acid (pH ∼2.5) showed a measured molecular weight of 6370 (Figure 2A), consistent for the apoprotein mass. The protein is not expected to bind zinc at this acidic pH due to the protonated state of the histidine ligands. NCp7 contains two zinc fingers, and at pH 6.9 in ammonium acetate (aqueous), the expected protein−Zn_2 species was detected as the major species (Figure 2b).

ESI-MS experiments were performed to monitor products from the reaction between NCp7−Zn_2 and selected 2,2′-dithiobis[benzamide] compounds. Two minutes after addition of 4 mol equiv of **2**, the major products were the [NCp7 + 2Zn] and [NCp7 + 266 +

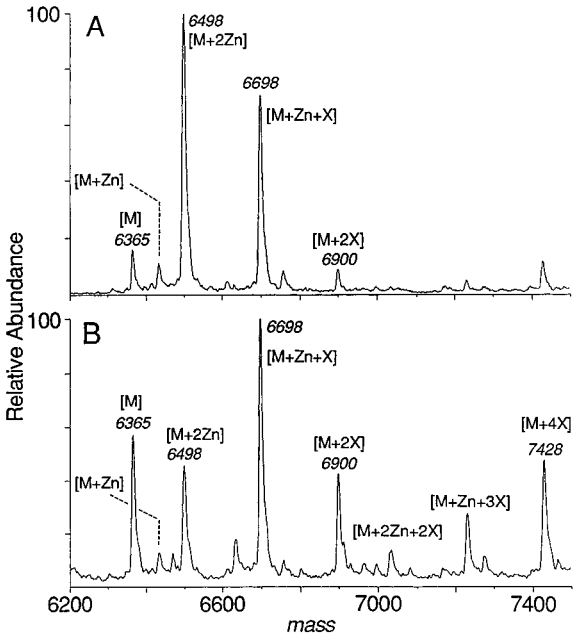

Figure 3. Time course study of Zn ejection from NCp7 by **2** as monitored by ESI-MS. Deconvoluted mass spectra taken 17 min (A) and 60 min (B) after 60 μM **2** was added to a solution containing 15 μM NCp7, 30 μM $ZnCl_2$, and 25 mM ammonium acetate, pH 6.9.

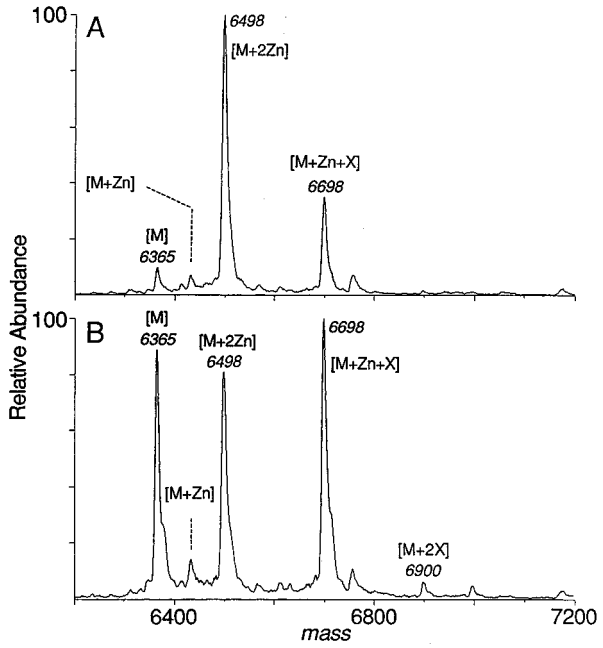

Figure 4. Time course study of Zn ejection from NCp7 by **3** as monitored by ESI-MS. Deconvoluted mass spectra taken 10 min (A) and 65 min (B) after addition of 60 μM **3** to a solution containing 15 μM NCp7, 30 μM $ZnCl_2$, and 25 mM ammonium acetate, pH 6.9.

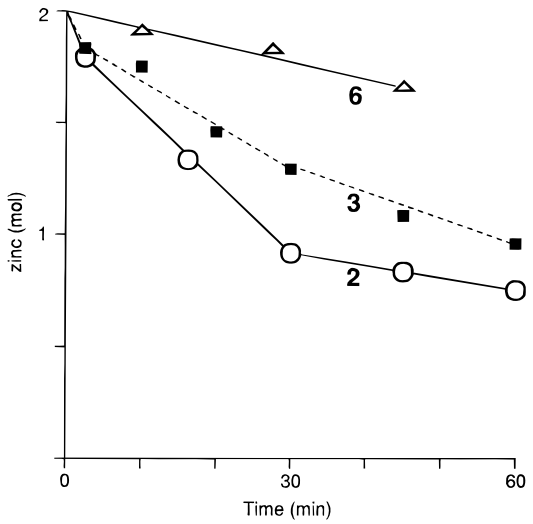

Figure 5. Time course study of total zinc ejection from NCp7 measured by MS. The absolute abundances (peak intensity) for each protein−zinc species were summed in each mass spectra acquired at each time point and normalized to the total protein ion signal. For example, all of the ion signals for the NCp7−Zn_1 species were counted together (i.e., [NCp7 + Zn] + [NCp7 + Zn + drug] + [NCp7 + Zn + 2drug] + etc.).

Zn] molecules, where 266 Da represents one-half of the 2,2′-dithiobis[benzamide] drug molecule. Some of the apoform (zinc-free protein) was also found at this time point. At later time periods, the apoprotein and its various covalently modified forms, e.g., [NCp7 + 2(266)], are the major products. Figure 3 shows the zinc ejection profile induced by **2** after 17 and 60 min.

Accurate high-resolution mass measurements indicate that up to a total of three intramolecular Cys−Cys bonds are formed upon zinc ejection. Each disulfide bond formation results in a net decrease of 2 Da relative to the fully reduced apoprotein. The measured molecular weight of some of the apoprotein formed by 2,2′-dithiobis[benzamide]-induced zinc ejection (6363.4 Da) was 6 Da less than the theoretical mass of the native protein (6369.5 Da). This is consistent with the report by Fenselau and co-workers,[3] who found that a total of three disulfide bonds formed upon oxidation of NCp7 by 3-nitrobenzamide.

For **3**, the benzisothiazolone form of **2**, only one adduct species was found in relatively large quantities, with release of zinc (Figure 4), whereas the 2,2′-dithiobis-[benzamide] **2** gave many more adduct species with different numbers of bound drug molecules (e.g., +1 drug molecule, +2, ...+6 drug molecules) (Figure 3). Figure 5 shows a time course plot of zinc ejection from NCp7 upon addition of compounds **2**, **3**, and **6** measured by ESI-MS. All of the protein species containing zero, one, and two zinc ions were added and normalized to the total protein signal. Both **2** and **3** showed moderate activity for zinc ejection in less than a 1 h time period, with the 2,2′-dithiobis[benzamide] form being slightly more active than the benzisothiazolone.

The sites of these covalent modifications during the early reaction stages (i.e., initial 10 min of reaction) were identified by analyzing proteolyzed fragments of NCp7−Zn_2 obtained by exposing the drug-treated protein to trypsin. From ESI-MS mass measurements, tandem mass spectrometry (MS/MS), and liquid chromatography-MS (LC-MS), the C-terminal zinc finger region was found to be more reactive with **2** than the N-terminal zinc finger. From limited trypsin digestion of drug-bound NCp7−Zn_2, separate tryptic peptides containing Cys36 and Cys49 were observed to be covalently modified by the drug. The MS data were not able to distinguish which of these two Cys residues reacts first with the drug. It is possible that Cys36 and Cys49 have nearly equal reactivity.

Characterization of Zn Ejection by NMR Spectroscopy. The utility of NMR spectroscopy to monitor

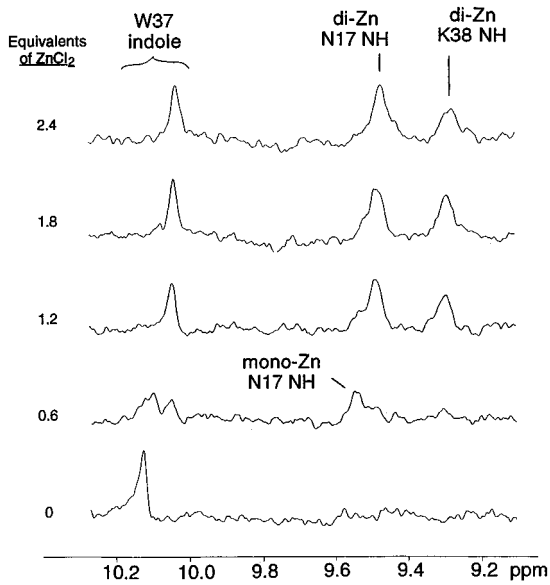

Figure 6. Titration of $ZnCl_2$ into a 0.5 mM solution of apo-NCp7 in 60 mM sodium phosphate, pH 7.4. The downfield amide proton region of the 500 MHz ^1H NMR spectrum is shown as a function of Zn/NCp7 ratio. Spectral assignments are indicated.

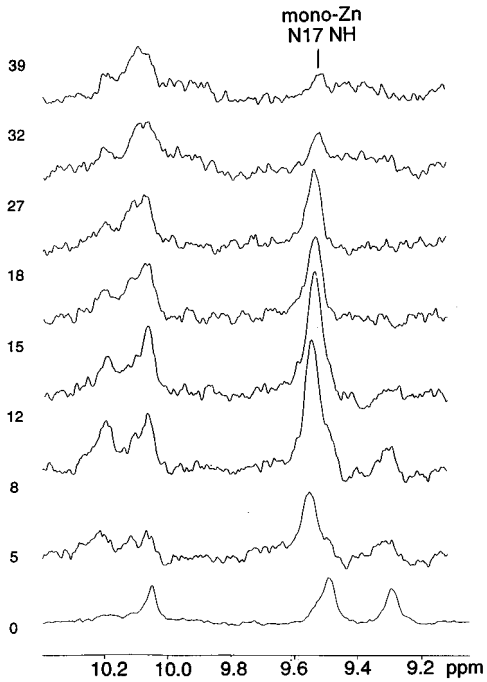

Figure 7. Time course of Zn ejection from NCp7 by **3** as monitored by ^1H NMR (downfield amide region). Spectra were run on 0.6 mM NCp7 samples dissolved in 60 mM sodium phosphate buffer, pH 7.4, at 25 °C. The bottom trace shows NCp7 in the absence of compound. From left to right, peak assignments are Trp37 indole, Asn17 NH, and Lys38 NH. Traces 2−6 show spectra recorded at the indicated times (in minutes) after addition of 2 equiv of **3**. Immediately after the 27 min spectrum was recorded, an additional 2 equiv of the compound was added, and the 32 and 39 min time points were acquired.

the ejection of zinc from NCp7 arises from the spectral dispersion in the proton NMR signals caused by the zinc finger structure. In particular, two amide proton signals are highly deshielded from the envelope of other peptide amide signals in the Zn-loaded peptide but not in apo-NCp7. These signals have been previously assigned to Asn17 (9.49 ppm) and Lys38 (9.28 ppm) in NCp7−Zn_2.[2,13,14] In order to better understand the NMR spectral changes occurring during Zn ejection, the reverse reaction was studied by titrating $ZnCl_2$ into a solution of apo-NCp7. Figure 6 shows the development of amide proton signals arising from the singly and doubly coordinated NCp7 as Zn is added. Two-dimensional TOCSY and NOESY experiments were used to make assignments. The observation of distinct resonances for the mono-Zn complex indicates that Zn coordination is noncooperative or negatively cooperative and is qualitatively consistent with the recently reported results of Mély et al.[15] Cooperative addition of Zn would require that occupation of a single Zn site in apo-NCp7 would increase the affinity for the second site. This would require that apo- or dicoordinated species would predominate at all Zn/peptide ratios ≤ 2. Crosspeaks at the Asn17 Hα and Hβ chemical shifts in the two-dimensional TOCSY spectrum recorded on a partially Zn-loaded sample of NCp7 (not shown) showed that the amide resonance assigned to the monocoordinated species is from Asn17. It can therefore be concluded that the N-terminal Zn finger of NCp7 is preferentially coordinated to generate a mono-Zn finger form of NCp7 at low Zn/peptide ratios. The chemical shift of the Trp37 indole proton is slightly different and shifted upfield on going from apo-NCp7 to NCp7−Zn to NCp7−Zn_2, and the chemical shift of Asn17 NH is slightly further downfield in NCp7−Zn than in NCp7−Zn_2. Since these two protons report on different Zn fingers, these results suggest some interaction does occur between the two Zn finger moieties under these conditions, as previously suggest by Morlett et al.[14,15] However, the observed chemical shift differences are small, and little can be ascertained about the nature of the interaction from this data.

The observation of spectral signals from each Zn finger allowed us to measure the relative sensitivity to 2,2′-dithiobis[benzamide]- and benzisothiazolone-induced metal ejection of each of the Zn fingers in intact NCp7. In one NMR experiment, 2 equiv of **3** were added to a solution of NCp7 and the ejection of Zn from each finger was followed by monitoring the loss of intensity of marker resonances from each finger (Figure 7). Experiments performed with **2** yielded similar results. In a different approach, **3** was titrated into a solution of NCp7 and the state of the peptide was monitored after each titration point had equilibrated, Figure 8. In all cases, we observed a loss in intensity of the resonances from Asn17 and Lys38 amide protons with concomitant growth of a resonance at a position previously assigned to Asn17 NH in mono-Zn NCp7, suggesting that Zn is ejected from the C-terminal Zn finger much faster than from the N-terminal Zn finger.

The expected structural changes upon Zn ejection based on the NMR spectroscopic observations described above led us to postulate that circular dichroism (CD) could be used to monitor Zn ejection from NCp7. The CD spectra of NCp7 before and after equilibration with **2** are shown in Figure 9. The pronounced changes observed in the CD spectrum are consistent with a loss of structural integrity in NCp7 upon treatment with **2** and removal of the Zn. The large $\Delta\epsilon$ at 220 nm allowed the time course of Zn ejection to be followed as a function of solution conditions. Temporal changes in ϵ220 of NCp7 upon addition of **2** are shown in Figure 9 at two

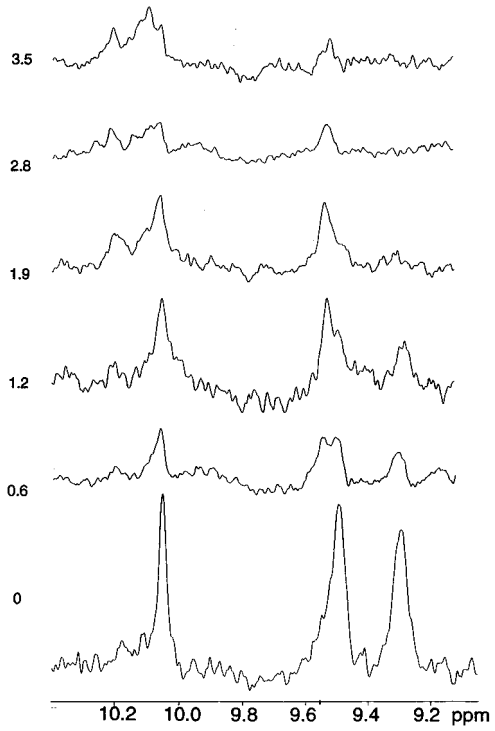

Figure 8. Titration of NCp7 with **3** as monitored by ^{1}H NMR (downfield amide region). Spectra were run on 0.3 mM NCp7 samples dissolved in 60 mM sodium phosphate, pH 7.4, at 25 °C. The bottom trace shows NCp7 in the absence of compound. From left to right, peak assignments are Trp indole, Asn17 NH, and Lys38 NH. Traces 2−6: after equilibrating with the indicated number of equivalents of **3**.

concentrations with a fixed 2,2′-dithiobis[benzamide]/NCp7 ratio of about 4. As indicated in Figure 9, these data required a minimum of two exponentials for a good fit.

Nonreactive 2,2′-Dithiobis[benzamide] Isostere. On the basis of the SAR of existing 2,2′-dithiobis-[benzamide] compounds,[4,7,8] it has been hypothesized that interactions of these agents with NCp7 could involve a prereaction complex in which the agent binds in a specific manner to a site on the peptide near the attacking Zn-liganded cysteine. One problem with identifying such an adduct is the relatively high reactivity of the 2,2′-dithiobis[benzamide] compounds. Because of the structural changes that NCp7 undergoes, the recognition complex would not be expected to survive Zn ejection. To see if a pre-ejection complex is formed, the interaction of a nonreactive thioether isostere of **2** (**6**) has been studied. Since peptide chemical shifts are sensitive to structural environs and because of the anisotropic nature of the aromatic groups in the compound, proton resonances from amino acids that interact with the compound should be shifted. The NH and Hα chemical shifts in NCp7 were recorded as a function of added **6** using TOCSY. In phosphate buffer at pH 5.9, there were no detectable shifts in the resonances of either **6** or Zn-loaded NCp7, even at a compound/NCp7 ratio of 6, suggesting that there is no substantial interaction between **6** and NCp7 under the NMR conditions. Furthermore, no new proton signals indicative of Zn ejection (e.g., Trp37 indole) appeared, suggesting that no Zn was ejected in solution.

Electrospray ionization mass spectra of NCp7 with **6** showed only a weak noncovalent adduct formed with

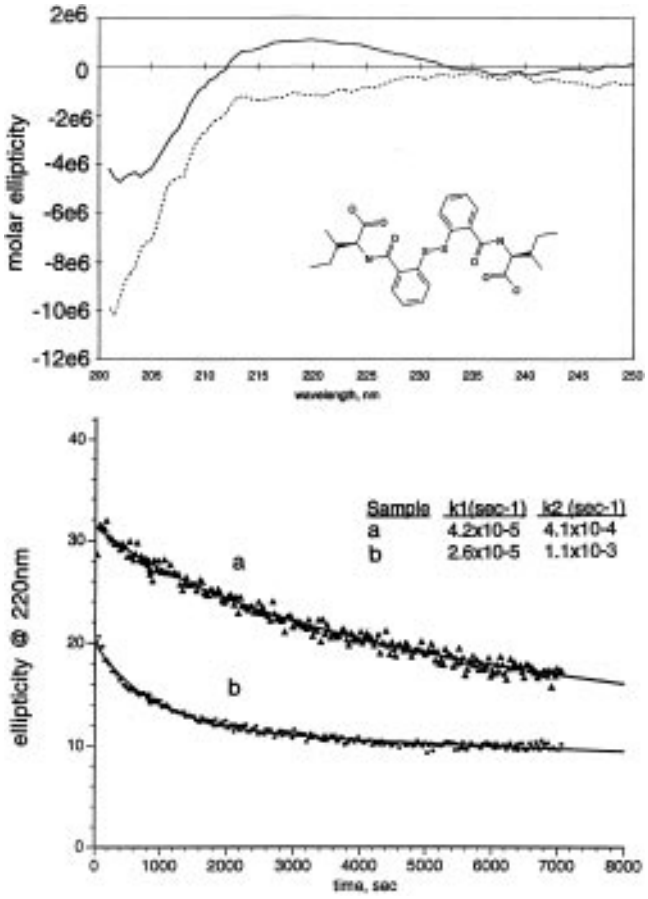

Figure 9. CD spectral changes in NCp7 as a result of treatment with **2**: (A) 30 μM NCp7 in 50 mM sodium phosphate, pH 7.0, at 25 °C before (—) and after (– – –) equilibration with 4.5 equiv of **2** and (B) time dependence of the ellipticity (at 220 nm) of NCp7 in phosphate buffer after addition of 4.5 equiv of **2** under the following conditions (a) 9.8 μM NCp7, pH 7.0, and (b) 73.4 μM NCp7, pH 7.0. Double-exponential fits to the time-dependent data are shown.

the NCp7−Zn_2 species that persisted over a 2 h period with very little ejection of zinc observed. The relative abundance of the [NCp7 + 2Zn + drug] ion was less than 20% of the [NCp7 + 2Zn] ion signal. Less than 0.2 equiv of zinc was ejected over the entire time monitored (Figure 5). On the basis of the lack of Zn ejection observed in the NMR solutions (see above), and the fact that **6** cannot act as an electrophile for Zn ejection, it is most likely that the small amount of Zn ejected in this experiment occurs due to interactions in the gas phase and cannot be interpreted as evidence for solution phase interactions. ESI-MS has demonstrated the capabilities to detect weakly bound macromolecular complexes. The ESI-MS experimental conditions used for this study were such that any specific noncovalent complexes would have been more prominent in the spectrum. The presence of the drug adduct is therefore most likely due to nonspecific interactions that may occur from the electrospray ionization process, e.g., adduct formation from the anionic **6** and the cationic NCp7 in the gas phase.

Discussion

NMR studies with the 2,2′-dithiobis[benzamide] **2** suggest that at physiologically relevant concentrations and pH, the monomeric thiol and benzisothiazolone forms of the compound represent significant populations

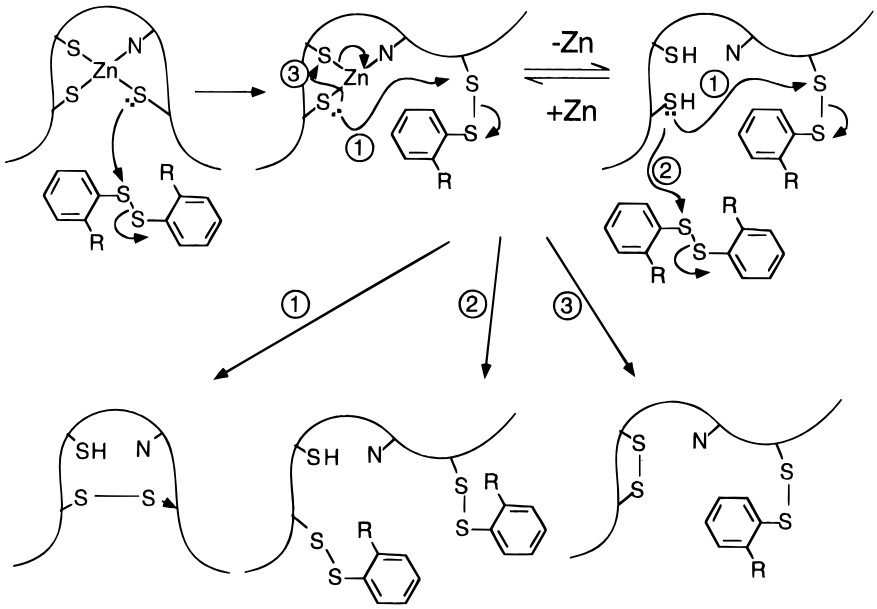

Figure 10. Possible reaction pathways in the interaction of 2,2′-dithiobis[benzamides] with NCp7.

in solution and that equilibrium between the various species is rapidly established. The benzisothiazolone **3**, on the other hand, is stable under these conditions in the absence of reducing agents. Both the 2,2′-dithiobis-[benzamide] and the benzisothiazolone are potential targets for nucleophilic attack, but the presence of benzisothiazolone in solutions of 2,2′-dithiobis[benzamide] makes it difficult to ascertain which is better at ejecting Zn. The different distribution of products observed in the mass spectra upon treatment with **2** and **3** suggests that both oxidized species do react with NCp7 via distinct mechanisms.

Our results clearly indicate that anti-HIV 2,2′-dithiobis[benzamides] cause Zn ejection from NCp7 in a stoichiometric, oxidative manner *in vitro*. Prominent among the final products of 2,2′-dithiobis[benzamides] or benzisothiazolones interacting with Zn-loaded NCp7 are drug−apoprotein adducts and internally disulfide-bonded apoprotein molecules. In terms of possible reaction mechanisms, the process can be viewed as an intermolecular disulfide formation followed by Zn ejection with concerted or subsequent intramolecular disulfide bond formation and/or rearrangement (Figure 10). First, a relatively slow nucleophilic attack of the oxidized (aromatic) sulfur by a Zn-coordinated cysteine sulfur atom results in a destabilization of the Zn coordination sphere. This is followed by (1) rapid formation of intramolecular disulfides within the protein and ejection of Zn or (2) rapid diffusion of Zn away from the protein followed by disulfide exchange. This view of the reaction mechanism is supported by the observation that peaks in the mass spectrum corresponding to [NCp7 + 2Zn + drug] are very low in abundance. The subsequent disulfide bond rearrangement stage occurs by formation of intramolecular (and possibly intermolecular) disulfide bonds involving cysteine sulfurs which are (or were previously) complexed to Zn. This disulfide formation could include attack of the mixed aromatic cysteine disulfide formed in the initial reaction by another electrophilic sulfur, with the aromatic sulfhydryl acting as a leaving group, or alternatively, attack of another aromatic 2,2′-dithiobis[benzamide], Figure 10.

On the basis of Zn ejection behavior as monitored by *N*-(6-methyl-8-quinolyl)-*p*-toluenesulfonamide (TSQ) and tryptophan fluorescence, it has been proposed that the kinetics of Zn ejection from the C-terminal finger are approximately 8-fold faster than from the N-terminal.[5] The similar biexponential rates of Zn ejection as measured by CD suggest that Zn ejection and protein unfolding are simultaneous events, since CD provides a direct measure of the rate of structural changes, whereas the TSQ fluorescence data measure the rate of liberation of Zn. That the C-terminal Zn finger ejects Zn faster is supported by the differential rates of disappearance of the amide protons associated with individual Zn fingers. By monitoring the same resonances going in the other direction, that is, adding Zn to apo-NCp7, it is clear that the N-terminal Zn site is occupied with higher affinity. This relative binding affinity was also observed with peptides that contained the individual Zn fingers.[11] In addition, the mass spectrometry data support the hypothesis that the C-terminal zinc finger is initially attacked by **2** or **3**. Thus it is clear that Zn is ejected slower from the more thermodynamically stable (N-terminal) Zn finger. It seems unlikely, however, that thermodynamic parameters drive the observed kinetics because once disulfide exchange occurs, the Zn finger cannot reform. Therefore, equilibrium cannot be established, and thermodynamic arguments are not applicable. An alternative explanation is that one of the C-terminal cysteine sulfurs is the most reactive nucleophile, which may or may not be related to the Zn-binding affinity for the individual fingers. The nucleophilicity of a particular cysteine could be due to electronic and/or steric considerations mandated by the secondary or tertiary structure of NCp7. Alternatively, if a recognition step is involved prior to electron transfer, then a C-terminal Zn finger recognition complex is expected to be more disposed to the initial electrophillic attack than an N-terminal complex. However, the data presented here with the nonreactive isostere **6**, while not conclusive evidence for the lack of a recognition complex, if taken with the apparent nonsaturable kinetic profile for similar compounds,[5] suggest that the existence of a

specific complex is unlikely. This being said, all of the Zn ejection studies mentioned heretofore have been conducted on naked NCp7 in the absence of RNA. It is entirely possible that recognition could be a factor within the NCp7−RNA−drug ternary complex.

In summary, we have shown that Zn ejection is associated with initial intermolecular disulfide bond formation between a Zn-liganded cysteine and the 2,2′-dithiobis[benzamide] compound. Large conformational changes in the peptide accompany Zn ejection, and the rate of ejection is faster for the C-terminal finger than the N-terminal finger. The fast Zn ejection rate is strongly concentration dependent, but both rates are independent of pH in the range of 6−7. It is clear that 2,2′-dithiobis[benzamide] and benzisothiazolone agents disrupt the structure of NCp7 by coordinating to Zn ligands within the peptide. It follows that the functional properties of the nucleocapsid are compromised by this perturbation, and this could provide the basis for inhibition of HIV infectivity. Although it is tempting to speculate that NCp7 is the relevant target for these compounds, their therapeutic efficacy and the absolute identification of their site of action await more rigorous cellular and *in vivo* testing.

Experimental Section

The expression and isolation of NCp7 protein was reported previously.[5] Synthesis of the three sulfur-containing compounds are described below.

[*S*-(*R,*R**)]-2-[[2-[[2-[(1-Carboxy-2-methylbutyl)carbamoyl]phenyl]disulfanyl]benzoyl]amino]-3-methylpentanoic Acid *tert*-Butyl Ester (1).** A solution of 10.0 g (53.2 mmol) of L-isoleucine *tert*-butyl ester in 100 mL of dichloromethane was treated with 5.6 g (55.0 mmol) of *N*-methylmorpholine. The resulting solution was cooled to 0 °C and treated rapidly dropwise with a solution of 8.3 g (24.2 mmol) of 2,2′-dithiobis-[benzoyl chloride][15] in 100 mL of dichloromethane, keeping the temperature below 0 °C. The mixture was stirred at 0 °C for 1 h and allowed to come to room temperature over 18 h. The solid was removed by filtration, washed with water, and dried *in vacuo* to give 6.5 g of **1,** mp 189−191 °C. The filtrate was washed with water, 0.5 M hydrochloric acid, and water, dried ($MgSO_4$), filtered, and evaporated *in vacuo* to give an additional 6.9 g of **1** of comparable purity. The combined fractions, 14.4 g, gave an overall yield of 86%: NMR (MeSO-d_6) δ 0.89 (t, 6H), 0.95 (d, 6H), 1.30 (m, 2H), 1.44 (s, 18H), 1.52 (m, 2H), 1.92 (m, 2H), 4.22 (t, 2H), 7.32 (t, 2H), 7.45 (t, 2H), 7.63 (dd, 4H), 8.76 (d, 2H); MS (*m*/*z* relative intensity) 645 (46, M^+), 322 (100, $^1/_2M^+$). Anal. ($C_{34}H_{48}N_2O_6S_2 \cdot 0.25H_2O$) C, H, N.

[*S*-(*R,*R**)]-2-[[2-[[2-[(1-Carboxy-2-methylbutyl)carbamoyl]phenyl]disulfanyl]benzoyl]amino]-3-methylpentanoic Acid (2).** A solution of 13.2 g (20.5 mmol) of the *tert*-butyl ester **1** in 50 mL of trifluoroacetic acid was stirred at room temperature for 18 h. The solvent was removed *in vacuo*, and the residue was dissolved in 50 mL of dichloromethane which was also removed *in vacuo*. The residue was triturated with 150 mL of ether/pentane (2:1), and the resulting solid was removed by filtration. After washing with 50 mL of ether/pentane (2:1) and pentane, the solid was dried *in vacuo* to give 9.9 g (91%) of **2**: mp 211−213 °C; NMR (MeSO-d_6) δ 0.82 (t, 6H), 0.90 (d, 6H), 1.25 (m, 2H), 1.45 (m, 2H), 1.89 (m, 2H), 4.29 (t, 2H), 7.25 (t, 2H), 7.40 (t, 2H), 7.59 (d, 4H), 8.68 (d, 2H), 12.63 (s, 2H); MS (*m*/*z* relative intensity) 531 (15, M − 1), 266 (100, $^1/_2M^+$). Anal. ($C_{26}H_{32}N_2O_6S_2$) C, H, N.

[*S*-(*R,*R**)]-3-Methyl-2-(3-oxo-3*H*-benz[*d*]isothiazol-2-yl)pentanoic Acid (3).** A stirred, room temperature suspension of 5.3 g (10.0 mmol) of **2** in 200 mL of dichloromethane was treated dropwise with 2.4 g (15.0 mmol) of liquid bromine. The reaction mixture was stirred at room temperature for 2 h and evaporated *in vacuo*. The residue was triturated with dichloromethane which was also evaporated *in vacuo* to remove excess bromine. The residue was partitioned between dichloromethane/5% sodium bicarbonate (200 mL of each). The aqueous layer was washed with dichloromethane and acidified to pH 1.5 with 6.0 M hydrochloric acid. After extracting with dichloromethane (2 × 75 mL), the combined organic layers were washed with water, dried ($MgSO_4$), filtered, and evaporated *in vacuo* to give 4.8 g (91%) of **3**: mp 50−52 °C; NMR (MeSO-d_6) δ 0.84 (t, 3H), 1.01 (d, 3H), 1.18 (m, 1H), 1.28 (m, 1H), 2.12 (m, 1H), 5.00 (d, 1H), 7.48 (t, 1H), 7.73 (t, 1H), 7.92 (dd, 2H); MS (*m*/*z* relative intensity) 264 (100, M − 1). Anal. ($C_{13}H_{15}NO_3S \cdot 0.25H_2O$) C, H, N.

2-[[(1-Carboxy-2-phenyl)sulfanyl]methyl]benzoic Acid (4). A solution of sodium ethoxide (6.8 g, 75 mmol) in ethanol (25 mL) and methyl 2-mercaptobenzoate (12.6 g, 75 mmol) was allowed to mix together for a period of 5 min, phthalide (10.0 g, 75 mmol) was added, and the solution was refluxed for an 18 h period. The resulting slurry was cooled, treated with a solution of KOH (10.0 g) in 33 mL of 10% aqueous ethanol, and heated to reflux for a 2 h period. The mixture was cooled and filtered, and the solid was washed with ethanol. The solid was dissolved in water, dilute HCl was added to pH 2, and the product was recovered by filtration. Recrystallization from hot acetic acid afforded 7.6 g (37%) of **4**: mp 256−257 °C; NMR (Me_2SO-d_6) δ 4.59 (s, 2H, S-CH_2-Ar), 7.19−7.23 (m, 1H, Ar), 7.37−7.39 (m, 1H, Ar), 7.41−7.56 (m, 5H, Ar), 7.85−7.89 (m, 1H, Ar); MS (*m*/*z*) 289 $(M + H)^+$. Anal. ($C_{15}H_{12}O_4S$) C, H, N.

[2*S*-[1[*R(*R**)],2*R**,3*R**]]-2-[[2-[[2-[(1-Carboxy-2-methylbutyl)carbamoyl]phenyl]sulfanyl]methyl]benzoyl]-amino]-3-methylpentanoic Acid (6).** A solution of **4** (1.6 g, 5 mmol) in thionyl chloride (20 mL) was heated to reflux for 4 h. The solution was cooled, concentrated under reduced pressure, and dried *in vacuo* at 40 °C to afford 1.6 g of crude acid chloride **5**. An ice-cooled solution of L-isoleucine *tert*-butyl ester, monohydrochloride (1.3 g, 5.0 mmol) and *N*-methylmorpholine (1.4 mL, 13 mmol) in dichloromethane (30 mL) was treated dropwise with the crude acid chloride **5** (0.8 g, 2.7 mmol) in dichloromethane (10 mL). The reaction mixture was allowed to warm to ambient temperature and mix for an additional 18 h. The solution was extracted with 5% citric acid, 8% $NaHCO_3$, and brine, dried with $MgSO_4$, and concentrated under reduced pressure. The residue was dissolved in dichloromethane (15 mL) containing anisole (1.5 mL) and treated with trifluoroacetic acid (15 mL). The solvents were removed after 6 h under reduced pressure and recrystallization from dichloromethane/ether/hexane afforded 0.9 g (77%) of **6**: mp 165−168 °C; NMR (Me_2SO-d_6) δ 0.79−0.92 (m, 12H, 4 CH_3), 1.18−1.33 (m, 2H, CH), 1.40−1.53 (m, 2H, CH), 1.85−1.88 (m, 2H, CH), 4.23−4.40 (m, 4H, S-CH_2, CH-CO_2), 7.23−7.40 (m, 8H, Ar), 8.44−8.47 (d, 1H, J = 3 Hz, NH), 8.52−8.55 (d, 1H, J = 3 Hz, NH), 12.6 (broad peak, 2H, CO_2H); MS (*m*/*z*) 513 $(M - H)^-$. Anal. ($C_{27}H_{34}N_2O_6S$) C, H, N.

NMR Spectroscopy. All NMR spectra were collected on a Bruker AMX500 spectrometer equipped with a thermostatically controlled ^{1}H-observed triple resonance probe. Two-dimensional total correlation (TOCSY) spectra[17] with 60 ms 7 kHz mlev-16[18] spin−lock fields and two-dimensional nuclear Overhauser (NOESY) spectra[19] were acquired at 298 or 288 K with 250 ms mixing times. All NMR spectra were processed using UXNMR (Bruker Instruments). For two-dimensional spectra, 1024 complex points were acquired in the t_2 dimension and 512 or 700 points in t_1. The data were zero-filled to a final matrix size of 2048 × 1024 points. Signal-to-noise was enhanced, and truncation artifacts were minimized by application of a $\cos^2$ function in both dimensions prior to Fourier transformation. One-dimensional spectra contained 16K complex points. Quadrature detection in the t_1 dimension was achieved by the TPPI method[20] in two-dimensional spectra.

Protein and thio compound samples were prepared by dissolving in 20−50 mM sodium phosphate buffer with warming at 37 °C and agitation if necessary. Solution pH's were checked and adjusted with dilute NaOH or HCl when necessary. Stock solutions of **2** and **3** (1−4 mM) were prepared by agitating and warming the buffer/compound mixture for 15 min at 37 °C, and these were monitored by ^{1}H NMR. The solution of the benzisothiazolone contained one species and

remained unchanged during the course of the experiment, whereas the 2,2′-dithiobis[benzamide] rapidly equilibrated to form monomer and benzisothiazolone (see above). The pH of reaction mixtures was verified before and after the reactions.

Mass Spectrometry. Positive ion ESI-MS analyses were performed with a Finnigan MAT 900Q forward geometry hybrid mass spectrometer (Bremen, Germany)[21] equipped with a position- and time-resolved ion-counting (PATRIC) focal-plane array detector[22] after the magnet and before the quadrupole analyzer. Mass spectra were acquired at full accelerating potential (5 kV) and a scan rate of 10 s decade^{-1}.

The electrospray ionization interface used was based on a heated glass capillary inlet.[23] Droplet desolvation was accomplished by a countercurrent stream of warm nitrogen (∼60 °C) and by energetic collisions in the electrospray interface. Sulfur hexafluoride coaxial to the spray was used to suppress corona discharges. Protein solutions for ESI-MS measurements were prepared at a concentration of 10−20 μM in 25 mM ammonium acetate (pH 6.9) with 2 times the protein molar concentration of $ZnCl_2$ in water. Stock solutions of the sulfur-containing compounds were prepared at a concentration of ca. 10 mM in MeOH. Sample solutions were infused through the ESI source at a flow rate of 1 μL min^{-1}.

Microbore LC-MS experiments with electrospray ionization were performed with a VG Micromass Trio-2000 single-quadrupole mass spectrometer and a Michrome Bioresources HPLC unit (Vydac C18 1 mm × 150 mm column).

Limited trypsin digestion of drug-bound NCp7 was performed by incubating the drug compound with NCp7−Zn_2 for 10 min in 25 mM ammonium acetate (pH 6.9) followed by the addition of trypsin (Promega, Madison, WI) to the 20% level (w/w). The reaction was quenched after 10 min with 0.1% (v/v) trifluoroacetic acid.

Acknowledgment. We gratefully acknowledge Drs. John Domagala, Donald Hupe, David Mack, David Moreland, and Peter Tummino for numerous insightful discussions and the assistance of Dr. Scott Buckel and Dana DeJohn in the proteolysis experiments.

Supporting Information Available: Tabulated chemical shifts for the aromatic and amide protons of **2**, **3**, and **7** (1 page). Ordering information is given on any current masthead page.

References

(1) Mély, Y.; Cornille, F.; Fournie-Zaluski, M. C.; Darlix, J. L.; Roques, R. P.; Gerard, D. Investigation of Zinc-Binding Affinities of Moloney Murine Leukemia Virus Nucleocapsid Protein and its Related Zinc Finger and Modified Peptides. *Biopolymers* **1991**, *31*, 899−906.

(2) Summers, M. F.; Henderson, L. E.; Chance, M. R.; Bess, J. W., Jr.; South, T. L.; Blake, P. R.; Sagi, I.; Perez-Alvarado, G.; Sowder, R. C., III; Hare, D. R.; Arthur, L. O. Nucleocapsid Zinc Fingers Detected in Retroviruses: EXAFS Studies of Intact Viruses and the Solution-State Structure of the Nucleocapsid Protein From HIV-1. *Protein Sci.* **1992**, *1*, 563−574.

(3) Yu, X.; Hathout, Y.; Fenselau, C.; Sowder, R. C., II; Henderson, L. E.; Rice, W. G.; Mendeleyev, J.; Kun, E. Specific Disulfide Formation in the Oxidation of HIV-1 Zinc Finger Nucleocapsid p7. *Chem. Res. Toxicol.* **1995**, *8*, 586−590.

(4) Domagala, J. M.; Bader, J. P.; Gogliotti, R. D.; Sanchez, J. P.; Stier, M. A.; Song, Y.; Vara Prasad, J. V. N.; Tummino, P. J.; Harvey, P.; Holler, T. P.; Gracheck, S.; Hupe, D.; Rice, W. G.; Schultz, R. The Structure Activity Relationships for a New Class of Anti HIV-1 Agents Targeted Toward Nucleocapsid Protein NCp7: The 2,2′-Dithiobisbenzamides. Unpublished manuscript.

(5) Tummino, P. J.; Scholten, J.; Harvey, P.; Holler, T. P.; Maloney, L.; Gogliotti, R.; Domagala, J. M.; Hupe, D. The *In Vitro* Ejection of Zinc From Human Immunodeficency Virus Type 1 Nucleocapsid Protein by Disulfide Benzamides With Cellular Anti-HIV Activity. *Proc. Natl. Acad. Sci. U.S.A.* **1996**, *93*, 969.

(6) Reily, M. D.; Loo, J. A. Biophysical Characterization of Zn Ejection from HIV Nucleocapsid Protein by Aromatic Disulfides. 3rd Conference on Retroviruses and Opportunistic Infections, Washington, DC, Jan. 28−Feb. 1, 1996; Abstract 339.

(7) Domagala, J.; Gogliotti, R.; Sanchez, J.; Stier, M.; Tummino, P.; Gracheck, S.; Hupe, D.; Bader, J.; Schultz, R.; Rice, W. Two Novel Classes of HIV-1 Inhibitors Which Interact With Nucleocapsid Protein p7NC: Structure Activity Relationships vs. Antiviral Activity and Correlation with Zn Ejection. 3rd Conference on Retroviruses and Opportunistic Infections, Washington, DC, Jan. 28−Feb. 1, 1996; Abstract 338.

(8) Rice, W. G.; Supko, J. G.; Malspeis, L.; Buckheit, R. W., Jr.; Clanton, D.; Bu, M.; Graham, L.; Schaffer, C. A.; Turpin, J. A.; Domagala, J.; Gogliotti, R.; Bader, J. P.; Halliday, S. M.; Coren, L.; Sowder, R. C., II; Arthur, L. O.; Henderson, L. E. Inhibitors of HIV Nucleocapsid Protein Zinc Fingers as Candidates for the Treatment of AIDS. *Science* **1995**, *270*, 1194−1197.

(9) Hu, P.; Ye, Q.-Z.; Loo, J. A. Calcium stoichiometry determination for calcium binding proteins by electrospray ionization mass spectrometry. *Anal. Chem.* **1994**, *66*, 4190−4194.

(10) Witkowska, H. E.; Shackleton, C. H. L.; Dahlman-Wright, K.; Kim, J. Y.; Gustafsson, J.-A. Mass spectrometric analysis of a native zinc-finger structure: the glucocorticoid receptor DNA binding domain. *J. Am. Chem. Soc.* **1995**, *117*, 3319−3324.

(11) Surovoy, A.; Waidelich, D.; Jung, G. Nucleocapsid protein of HIV-1 and its Zn^{2+} complex formation analysis with electrospray mass spectrometry. *FEBS Lett.* **1992**, *311*, 259−262.

(12) Fenselau, C.; Yu, X.; Bryant, D.; Bowers, M. A.; Sowder, R. C., II; Henderson, L. E. Characterization of processed gag proteins from highly replicating HIV-1MN. In *Mass Spectrometry for the Characterization of Microorganisms*; Fenselau, C., Ed.; ACS Symposium Series; American Chemical Society: Washington, DC, 1994; pp 159−172.

(13) Omichinski, J. G.; Clore, G. M.; Sakaguchi, K.; Appella, E.; Gronenborn, A. M. Structural Characterization of a 39-residue Synthetic Peptide Containing the Two Zinc Binding Domains From the HIV-1 p7 Nucleocapsid Protein by CD and NMR Spectroscopy. *FEBS Lett.* **1991**, *292*, 25−30.

(14) Morellet, N.; de Rocquigny, H.; Mély, Y.; Jullian, N.; Déméné, H.; Ottmann, M.; Gérard, D.; Darlix, J. L.; Fournie-Zaluski, M. C.; Roques, B. P. Conformational Behavior of the Active and Inactive Forms of the Nucleocapsid NCp7 of HIV-1 Studied by ^{1}H NMR. *J. Mol. Biol.* **1994**, *235*, 287−301.

(15) Mély, Y.; De Rocquigny, H.; Morellet, N.; Roques, B. P.; Gerard, D. Zinc Binding to the HIV-1 Nucleocapsid Protein: A Thermodynamic Investigation by Fluorescence Spectroscopy. *Biochemistry* **1996**, *35*, 5175−5182.

(16) Collman, J. P.; Groh, S. E. "Mercaptan-Tail" Porphyrins: Synthetic Analogues for the Active Site of Cytochrome P-450. *J. Am. Chem. Soc.* **1982**, *104*, 1391−1403.

(17) Braunschweiler, L.; Ernst, R. R. Coherence Transfer by Isotropic Mixing: Application to Proton Correlation Spectroscopy. *J. Magn. Reson.* **1983**, *53*, 521−528.

(18) Bax, A.; Davis, D. G. MLEV-17-Based Two-Dimensional Homonuclear Magnetization Transfer Spectroscopy. *J. Magn. Reson.* **1985**, *65*, 355−360.

(19) Kumar, A.; Ernst, R. R.; Wüthrich, K. A two-dimensional nuclear Overhauser enhancement (2D NOE) experiment for the elucidation of complete proton-proton cross-relaxation networks in biological macromolecules. *Biochem. Biophys. Res. Commun.* **1980**, *95*, 1−6.

(20) Marion, D.; Wüthrich, K. Application of phase sensitive two-dimensional correlated spectroscopy (COSY) for measurements of proton-proton spin-spin coupling constants in proteins. *Biochem. Biophys. Res. Commun.* **1983**, *113*, 967−974.

(21) Loo, J. A.; Ogorzalek Loo, R. R.; Andrews, P. C. Primary to quaternary protein structure determination with electrospray ionization and magnetic sector mass spectrometry. *Org. Mass Spectrom.* **1993**, *28*, 1640−1649.

(22) Loo, J. A.; Pesch, R. Sensitive and selective determination of proteins with electrospray ionization magnetic sector mass spectrometry and array detection. *Anal. Chem.* **1994**, *66*, 3659−3663.

(23) Fenn, J. B.; Mann, M.; Meng, C. K.; Wong, S. F.; Whitehouse, C. M. Electrospray ionization for mass spectrometry of large biomolecules. *Science* **1989**, *246*, 64−71.

JM960253W